

## Stability mechanism of cuboctahedral clusters in $\text{UO}_{2+x}$ : First-principles calculations

Hua Y. Geng, Ying Chen, and Yasunori Kaneta

Department of Quantum Engineering and Systems Science, The University of Tokyo, Hongo 7-3-1, Tokyo 113-8656, Japan

Motoyasu Kinoshita

Nuclear Technology Research Laboratory, Central Research Institute of Electric Power Industry, Tokyo 201-8511, Japan  
and Japan Atomic Energy Agency, Ibaraki 319-1195, Japan

(Received 3 March 2008; revised manuscript received 21 April 2008; published 20 May 2008)

The stability mechanism of cuboctahedral clusters in nonstoichiometric uranium dioxide is investigated by first-principles local density approximation with Hubbard correction method. Calculations reveal that the structural stability is inherited from  $\text{U}_6\text{O}_{12}$  molecular cluster, whereas the energy gain through occupying its center with an additional oxygen makes the cluster win out by competition with point oxygen interstitials. Local displacement of the center oxygen along the  $\langle 111 \rangle$  direction also leads the cluster eightfold degeneracy and increases relatively the concentration at finite temperatures. However, totally, elevation of temperature, i.e., the effect of entropy, favors point interstitial over cuboctahedral clusters.

DOI: 10.1103/PhysRevB.77.180101

PACS number(s): 61.72.J-, 71.15.Nc, 71.27.+a

Uranium dioxide adopts the simple fluorite ( $\text{CaF}_2$ ) type of crystal structure with a space group  $Fm\bar{3}m$ . However, its self-defects, as in most anion excess fluorites, exhibit rather complex behavior: experimentally oxygen interstitials do not occupy the largest cation octahedral hole ( $\frac{1}{2}, \frac{1}{2}, \frac{1}{2}$ ) but form low symmetric clusters composed of oxygen vacancies instead.<sup>1-3</sup> The exact geometry of these clusters, however, is unclear. Experimentalists have proposed several structural models to explain the measured neutron diffraction patterns,<sup>3,4</sup> of which the cuboctahedral cluster (COT) appearing in  $\text{U}_4\text{O}_9$  (Refs. 5 and 6) and  $\text{U}_3\text{O}_7$  (Refs. 7 and 8) is the most clearly described. However, even with this structure, ambiguity remains about whether the center is occupied by an additional oxygen (COT-*o*) or not (COT-*v*),<sup>7</sup> and if the center atom really displaced off-center along the  $\langle 111 \rangle$  direction in the case that it was occupied.<sup>5,6</sup> Theoretical analysis has been little help so far since most of the work was confined to point oxygen interstitial ( $\text{O}_i$ ) and vacancy ( $\text{O}_v$ ) where the former always sites at the octahedral hole and thus failed to explain the experimental phenomena.<sup>9-11</sup> Inspired by its close relationship with Willis-type clusters, it was suggested that COT should also be present in  $\text{UO}_{2+x}$ .<sup>4,9</sup> A fully understanding of its property and stability mechanism thus becomes important not only for a general description of fluorite-related clusters<sup>12</sup> but also for nuclear applications, for example, the safe disposal of used nuclear fuel where the formation of  $\text{U}_4\text{O}_9/\text{U}_3\text{O}_7$  is a key process for the development of  $\text{U}_3\text{O}_8$  phase, which can lead to splitting of the sheath.<sup>13</sup>

Historically, COT was denoted by  $\text{M}_6\text{X}_{36}$  (or  $\text{M}_6\text{X}_{37}$  if an additional anion occupies the center).<sup>5,12</sup> It is a little misleading since the actual defect is composed of only 12 interstitials [forming the cuboctahedral geometry, see Fig. 1(a)] and eight vacancies [forming the small cube in Fig. 1(a)]. Different from Willis-type clusters whose stability can be interpreted in a similar concept of split-interstitial defect where several atoms share the common lattice sites,<sup>9</sup> COT is of more regular and with higher symmetry [point group  $\text{O}_h(m\bar{3}m)$ ], and poises as the special one. In fact, our calcu-

lations that will be reported here revealed it is actually a  $\text{U}_6\text{O}_{12}$  molecular cluster incorporated in bulk fluorite  $\text{UO}_2$  by sharing the uranium atoms with the cation sublattice face centers [Figs. 1(a) and 1(b)] after removing the eight corresponding lattice oxygens from the matrix. Thus, the inserted 12 oxygens presented as Willis  $\text{O}'$  interstitials that displaced along the  $\langle 110 \rangle$  directions in the picture of fluorite structure.

In calculations, COT cluster was modeled by embedding it into a cubic supercell of fluorite  $\text{UO}_2$  with otherwise 96 atoms ( $\text{U}_{32}\text{O}_{64}$ ). This configuration has large enough cell size with a deviation composition  $x = \frac{1}{8}$  for COT-*v* and  $\frac{5}{32}$  for

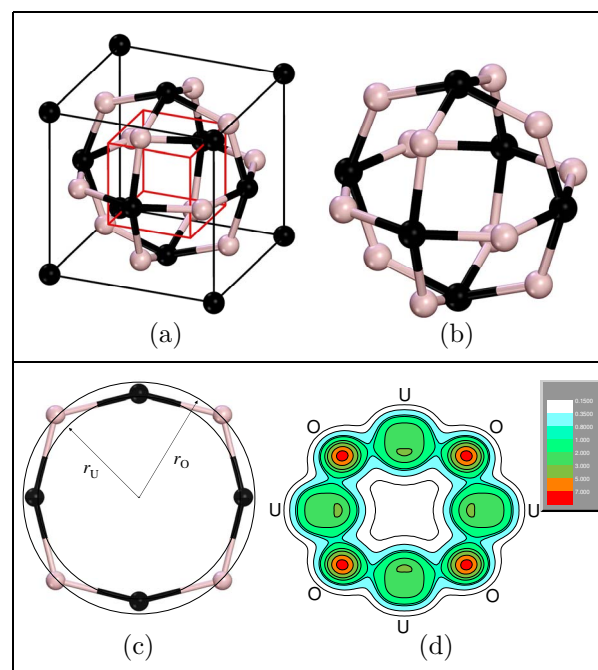


FIG. 1. (Color online) (a) Cuboctahedral cluster (COT-*v*) incorporated in a fluorite cell, where the small inner cube indicates the (removed) oxygen cage. (b)  $\text{U}_6\text{O}_{12}$  molecular cluster. (c) One of the three mutually perpendicular U-O rings in  $\text{U}_6\text{O}_{12}$  cluster, and (d) its charge density.

TABLE I. First-principles results for structural and energetic properties of oxygen defects in uranium dioxide:  $x$  is the deviation from the stoichiometric composition,  $\Delta V$  the defect induced volume change that averaged to per fluorite cubic cell,  $r_U$  and  $r_O$  the structural parameters of cuboctahedral cluster as indicated in Fig. 1(c),  $L$ ,  $\widehat{UOU}$ , and  $\widehat{OUO}$  are the averaged nearest neighbor bond length between U and O atoms, and the corresponding angles in cuboctahedral cluster, respectively;  $E_f$ ,  $E_{ef}$ , and  $E_{pf}$  are the overall defect formation energy, formation energy per excess oxygen, and per oxygen Frenkel pair, respectively.

	$x$	$\Delta V$ ( $\text{\AA}^3$ )	$r_U$ ( $\text{\AA}$ )	$r_O$ ( $\text{\AA}$ )	$L$ ( $\text{\AA}$ )	$\widehat{UOU}$ (deg)	$\widehat{OUO}$ (deg)	$E_f$ (eV)	$E_{ef}$ (eV)	$E_{pf}$ (eV)
$U_6O_{12}$	0		2.54	2.87	2.09	118.3	151.7			
COT- $v$	$\frac{1}{8}$	-0.14	2.92	2.82	2.20	139.7	129.8	-7.18	-1.80	1.91
COT- $o$	$\frac{5}{32}$	-1.61	2.76	2.90	2.18	127.9	141.6	-12.41	-2.48	1.94
COT <sup>a</sup>	0.21	-1.95	2.79	2.93	2.20	127.9	141.5			
$O_i^b$	$\frac{1}{32}$	-0.29						-2.17	-2.17	5.36
$O_v^b$	$-\frac{1}{32}$	0.20						7.53		5.36

<sup>a</sup>Experiment of  $\beta$ - $U_4O_9$  at 503 K reported in Ref. 6.

<sup>b</sup>Isolated point defects (Ref. 9).

COT- $o$  compared to experimental  $x \approx 0.21$  for  $U_4O_9$  (Ref. 6) and 0.35 for  $U_3O_7$ ,<sup>7</sup> respectively.  $U_6O_{12}$  molecular cluster was modeled by putting into a vacuum cubic box with a lateral length of 11  $\text{\AA}$ , a sufficient distance for the current purpose. Total energies were calculated with plane wave method based on density functional theory,<sup>14</sup> with generalized gradient approximation (GGA) (for  $U_6O_{12}$ ), local density approximation with Hubbard correction<sup>15,16</sup> (for COTs) and projector-augmented wave pseudopotentials.<sup>17,18</sup> All structures have been fully relaxed to get all forces and stress less than 0.01 eV/ $\text{\AA}$ . Other computational parameters such as the kinetic energy cutoff and sampling  $k$  points are the same as those in Ref. 9, which focused on point defects behaviors.

The uraniums in COTs that embedded in  $UO_2$  are found always bond to interstitial oxygens first with a shorter bond length than to the nearest neighbor (NN) lattice oxygens (2.2 vs 2.4  $\text{\AA}$ ). Analysis of electronic density also shows the weak covalent bonds that forming an  $U_6O_{12}$  cluster are always prior to other bonds [Fig. 1(d)]. Local distortions have not changed the picture and preserve much of the tightly connected feature of vacuum  $U_6O_{12}$  cluster, which consists of three mutually perpendicular U-O rings that in turn determined by the two radius from the cluster center to the uranium ( $r_U$ ) and oxygen ( $r_O$ ) atoms completely, as shown in Fig. 1(c). Vacuum  $U_6O_{12}$  is perfect and without any deformation freedom such as variation in U-O bond length and related angles. All real but low vibrational frequencies (not shown here) indicate that the structure is locally stable but flexible for distortion. A cohesive energy of 21.2 eV/ $UO_2$  molecule is comparable to the bulk material [22.3 (23.9) eV of experiment (GGA)].<sup>19</sup> These features and the geometry make  $U_6O_{12}$  can be incorporated naturally with fluorite crystal (or generally, fcc lattice) and forms COT clusters without disturb the host structure severely.

Locally, COTs repulse the NN lattice oxygens outward slightly, but no evident distortion on cations was observed. As listed in Table I, the overall volume is contracted but the cube that contains the COT is expanded greatly, with a lateral length of  $2r_U$ . Also, embedding  $U_6O_{12}$  into  $UO_2$  not only

swells the cube (with an increased  $r_U$  and  $r_O$ ) but also leads to other local distortions. Usually, the distorted U-O ring is not on the same plane any longer and has additional freedoms in U-O bond length ( $L$ ) and related angles ( $\widehat{UOU}$  and  $\widehat{OUO}$ ). Their averaged values are listed in Table I compared to vacuum  $U_6O_{12}$  and experimental estimates of COT measured at 503 K on  $\beta$ - $U_4O_9$ .<sup>6</sup> Obviously, COT- $o$  agrees with the experimental one much better than COT- $v$  in geometry. With an additional oxygen occupied the center, COT- $o$  decreases the values of  $r_U$  and  $\widehat{UOU}$  while lifts  $r_O$  and  $\widehat{OUO}$  significantly with respect to COT- $v$ , identifying it as the one that appeared in experiments.

In contrast to the symmetry anticipation,<sup>5</sup> the center oxygen in COT- $o$  does not site at the *real* center. It displaces along the  $\langle 111 \rangle$  direction of fluorite structure with a distance about 0.43  $\text{\AA}$  compared well to Cooper and Willis' estimate of 0.64  $\text{\AA}$  (Ref. 6) and stands as an  $O''$  interstitial. In vacuum  $U_6O_{12}$  cluster, such kind of off-center displacement is forbidden. The small  $r_U$  ensures the energy minimum always at the cluster center. However, the  $r_U$  of COTs are enlarged by bulk  $UO_2$  matrix, which in turn shifts the energy minimum off center. By displacing the center oxygen along the  $\langle 111 \rangle$  direction, the three NN uraniums within the corresponding section of the COT shell are pulled inward  $\sim 0.2$   $\text{\AA}$  (while the three oxygens are pushed out slightly  $\sim 0.1$   $\text{\AA}$ ) and reduced the U-O bond length from 2.76 to 2.44  $\text{\AA}$ . The  $O_h(m\bar{3}m)$  symmetry is also broken to  $C_{3v}(3m)$ . In contrast, the symmetry broken in COT- $v$  is mainly due to Jahn-Teller distortion, where one uranium atom out relaxed but another five shift inward, results in a  $C_{4v}(4mm)$  symmetry.

The large cohesive energy of  $U_6O_{12}$  leads to a deep formation energy of COT clusters, as indicated in Table I, where the energetic information of isolated point defects ( $O_i$  and  $O_v$ ) are also given for comparison. By compensating excess oxygens with point vacancies, we find the formation energy per Frenkel pair in COT is just one-third of the isolated case. However, the energy gain for each excess oxygen exhibits different behaviors for COT- $v$  and COT- $o$ . With the contribution of the center oxygen, the latter has a lower  $E_{ef}$  than the point interstitial but the former is weighed down by the

electronic density cavity presented in the cluster center which costs the energy significantly.

With regard to the concentration of COT at finite temperatures, an intuitive picture is that it should favor moderate temperatures since otherwise there have not sufficient vacancies to facilitate the formation of the cluster. However, as mentioned above, the vacancies in COT actually are not from point defects but inherited integrally from the  $U_6O_{12}$  molecular cluster, this naive picture thus becomes invalid. To calculate the defect concentrations at finite temperatures properly, we employed here the independent clusters approximation (a generalization of the point defect model),<sup>9,20,21</sup> in which all involved clusters are assumed to be thermodynamically independent and obey Boltzmann distribution. In closed regime where no particle exchange with the exterior occurs, the concentration  $\rho_i$  of cluster  $i$  that has an internal degeneracy  $g_i$ ,  $n_i$  excess oxygens, and a formation energy  $E_f^i$  is given by

$$\rho_i [V_O]^{n_i} = g_i \exp\left(\frac{-E_f^i - n_i \times E_f^{O_v}}{\kappa_B T}\right). \quad (1)$$

Here,  $n_i$  point oxygen vacancies ( $O_v$ ) have been introduced as compensations. Therefore, we have a system that contains point oxygen (uranium) defects (treated as intrinsic Frenkel pairs), COT- $v$  and COT- $o$  clusters, which compete to each other. The oxygen and uranium subsystems are coupled up via the isolated point Schottky defects.<sup>9</sup> Among these defects, only COT- $o$  has an internal freedom with eightfold degeneracy ( $g=8$ ) arising from the  $\langle 111 \rangle$  direction displacement of the center oxygen and all others have  $g=1$ . COT- $v$  has four and COT- $o$  has five excess oxygen. At a composition  $x$  deviated from the stoichiometry, Eq. (1) is under a constraint of

$$x = 2([V_U] - [I_U]) + [I_O] + \sum_i n_i \rho_i - 2[V_O], \quad (2)$$

where the quantities in brackets denote point defect concentrations and  $i$  runs over COT- $v$  and COT- $o$  clusters, with a coefficient equals to the corresponding  $n_i$  because each octahedral hole of the cation sublattice defines not only a point interstitial site but also a COT- $v(o)$  cluster.

Using the calculated first-principles formation energies, we get the defect concentrations as a function of temperature and composition by solving Eqs. (1) and (2). The hypostoichiometric regime is always dominated by  $O_v$  and thus trivial. Interesting competition between defects appears on the other section of composition with  $x > 0$ . The solid lines in Fig. 2 show the equilibrium concentrations of point oxygen interstitial  $O_i$ , uranium vacancy  $U_v$ , and COT- $o$  cluster at a temperature of 1500 K around this regime. All other defects have a concentration of 10 more orders smaller and not shown here.  $O_i$  is predominant at low  $x$  with a rapid increment of its concentration, which flattens out gradually at high compositions. By contrast, COT- $o$  approaches a linear dependence on composition after  $x > 0.025$  and dominates the regime of  $x > 0.1$ . The overall concentration of  $U_v$  is 1 order smaller than  $O_i$  and has dismissed its influence on material properties.

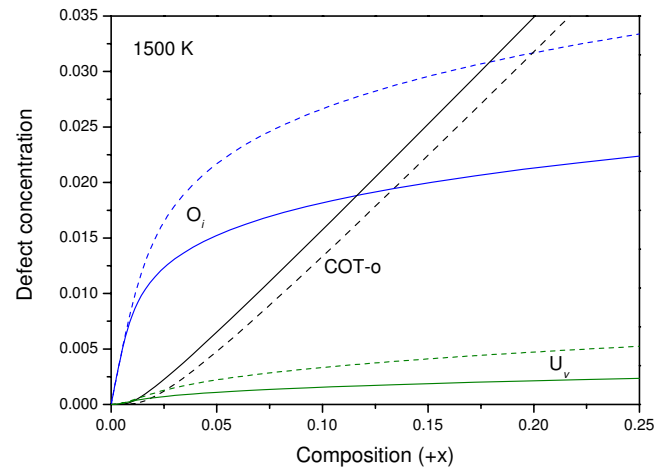


FIG. 2. (Color online) Defect concentrations of point oxygen interstitial, uranium vacancy, and COT- $o$  cluster. The dashed lines indicate the corresponding results where the center oxygen in COT- $o$  has no off-center displacement and thus with  $g=1$ .

The predominance of COT- $o$  over COT- $v$  is due to the energy gain of the center oxygen but not the entropy contribution of the eightfold state. The dashed lines in Fig. 2 give the corresponding concentrations by treated COT- $o$  with  $g=1$ . Removal of the internal entropy contribution do reduce the competitiveness of COT- $o$  and increase the concentration of  $O_i$  greatly, as well as that of  $U_v$ , but has not changed the picture qualitatively—the concentration of COT- $v$  is still 10 more orders smaller. Conversely, if rescale the formation energy of COT- $o$  so that it has the same  $E_{ef}$  as COT- $v$ , then they will have comparable concentrations, but of 10 orders smaller than that of  $O_i$ .

Figure 3 shows the variation of defects competition along temperature from 500 to 1500 K. The solid (dotted) line indicates the oxygen interstitial (vacancy) concentration arising from COT clusters: each COT- $o(v)$  contributes 13(12) oxygen interstitials and eight vacancies. It is obvious that temperature increase, i.e., the entropy effect, favors point

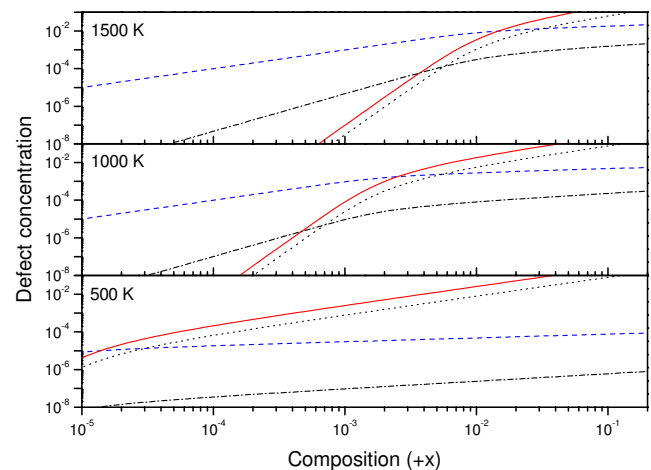


FIG. 3. (Color online) Defect concentrations at different temperatures: solid (dotted) line—oxygen interstitial(vacancy) arising from COTs, dashed line—point oxygen interstitial, and dash-dotted line—point uranium vacancy. All other components are negligible.

defects over COT clusters greatly. The predominant range of  $O_i$  has increased 3 orders by elevating the temperature from 500 to 1500 K. All point defect concentrations are enhanced along this process except those from COT clusters, which are reduced by temperature. This is because the probability to form a COT-*o* cluster from point defects is proportional to  $[I_O]^{13}[V_O]^8$  but each COT-*o* in conversely contributes only 13(8) interstitials(vacancies), showing point defect is more disordered and with larger entropy.

Figure 3 demonstrates that at 500 K, COT-*o* is the exclusive defect cluster and support the empirical assumption that  $\beta$ - $U_4O_9$  contains only this kind of cluster.<sup>6</sup> From the temperature dependence of defect concentrations, we can be sure that the lower temperature  $\alpha$  phase also should contain COT-*o* exclusively. On the other hand, the current interpretation of the neutron diffraction pattern in  $U_3O_7$  is questionable, which employed COT-*v* instead of COT-*o* cluster.<sup>7</sup> The former has a negligible concentration of 10 more orders smaller and thus invalidates the analysis definitely. The ordering of the clusters that distributed in these phases,<sup>8</sup> how-

ever, seems should be driven by long-ranged strain energy rather than by chemical interactions. By the volume change induced by defects listed in Table I and the fact that COT itself expands the occupied fluorite cube seriously, there is a strong deformation field around each COT cluster, which repulses other COTs away. The stress magnitude can be estimated from the bulk modulus of  $UO_2$  as  $\sim 2$  GPa, a high enough value and any off-balance happened on the boundaries of deformed domains will lead to cracks. That is why  $U_4O_9/U_3O_7$  film cannot protect  $UO_2$  pellet from being oxidized effectively.<sup>13</sup> Such cracks are also believed as the onset of high burn-up structures in nuclear fuels where uraniums are highly consumed and deteriorates the fuel quality severely.<sup>22</sup>

Support from the Budget for Nuclear Research of the Ministry of Education, Culture, Sports, Science and Technology of Japan based on the screening and counseling by the Atomic Energy Commission is acknowledged.

- 
- <sup>1</sup>B. T. M. Willis, *J. Phys. (France)* **25**, 431 (1964).  
<sup>2</sup>B. T. M. Willis, *Proc. Br. Ceram. Soc.* **1**, 9 (1964).  
<sup>3</sup>B. T. M. Willis, *Acta Crystallogr., Sect. A: Cryst. Phys., Diffraction, Theor. Gen. Crystallogr.* **A34**, 88 (1978).  
<sup>4</sup>A. D. Murray and B. T. M. Willis, *J. Solid State Chem.* **84**, 52 (1990).  
<sup>5</sup>D. J. M. Bevan, I. E. Grey, and B. T. M. Willis, *J. Solid State Chem.* **61**, 1 (1986).  
<sup>6</sup>R. I. Cooper and B. T. M. Willis, *Acta Crystallogr., Sect. A: Found. Crystallogr.* **A60**, 322 (2004).  
<sup>7</sup>F. Garrido, R. M. Ibberson, L. Nowicki, and B. T. M. Willis, *J. Nucl. Mater.* **322**, 87 (2003).  
<sup>8</sup>L. Nowicki, F. Garrido, A. Turos, and L. Thome, *J. Phys. Chem. Solids* **61**, 1789 (2000).  
<sup>9</sup>H. Y. Geng, Y. Chen, Y. Kaneta, M. Iwasawa, T. Ohnuma, and M. Kinoshita, *Phys. Rev. B* **77**, 104120 (2008).  
<sup>10</sup>J. P. Crocombette, F. Jollet, T. N. Le, and T. Petit, *Phys. Rev. B* **64**, 104107 (2001).  
<sup>11</sup>M. Freyss, T. Petit, and J. P. Crocombette, *J. Nucl. Mater.* **347**, 44 (2005).  
<sup>12</sup>D. J. M. Bevan and S. E. Lawton, *Acta Crystallogr., Sect. B: Struct. Sci.* **B42**, 55 (1986).  
<sup>13</sup>R. J. McEachern and P. Taylor, *J. Nucl. Mater.* **254**, 87 (1998).  
<sup>14</sup>G. Kresse and J. Furthmüller, *Phys. Rev. B* **54**, 11169 (1996).  
<sup>15</sup>V. I. Anisimov, J. Zaanen, and O. K. Andersen, *Phys. Rev. B* **44**, 943 (1991).  
<sup>16</sup>V. I. Anisimov, I. V. Solovyev, M. A. Korotin, M. T. Czyzyk, and G. A. Sawatzky, *Phys. Rev. B* **48**, 16929 (1993).  
<sup>17</sup>P. E. Blöchl, *Phys. Rev. B* **50**, 17953 (1994).  
<sup>18</sup>G. Kresse and D. Joubert, *Phys. Rev. B* **59**, 1758 (1999).  
<sup>19</sup>H. Y. Geng, Y. Chen, Y. Kaneta, and M. Kinoshita, *Phys. Rev. B* **75**, 054111 (2007).  
<sup>20</sup>Hj. Matzke, *J. Chem. Soc., Faraday Trans. 2* **83**, 1121 (1987).  
<sup>21</sup>A. B. Lidiard, *J. Nucl. Mater.* **19**, 106 (1966).  
<sup>22</sup>J. Noirot, L. Desgranges, and J. Lamontagne, *J. Nucl. Mater.* **372**, 318 (2008).